



Structural Analysis with Augmented Optoelectronic Performance of Polyindole–Polypyrrole–Cadmium Sulfide Nanohybrid: PIN/PPY/CdS

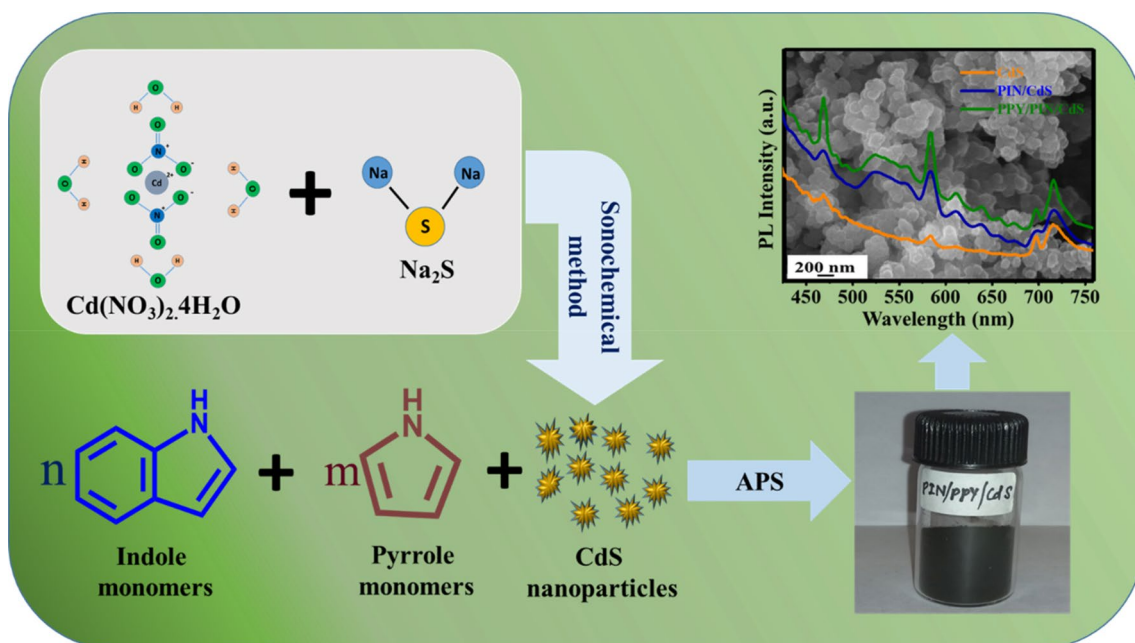
Ajeet Verma¹ · Ram Bilash Choudhary¹ · Debashish Nayak¹ · Gobind Mandal¹

Received: 4 November 2019 / Accepted: 29 March 2020 / Published online: 12 April 2020
© Springer Science+Business Media, LLC, part of Springer Nature 2020

Abstract

We report the comparative morphological, structural and optoelectronic properties of ternary PIN/PPY/CdS nanohybrid material synthesized by chemical oxidative polymerization technique. The successful incorporation of CdS nanoparticles into polymeric PIN and PIN/PPY matrix was confirmed by X-ray diffraction (XRD) and Fourier transform infrared spectroscopic (FT-IR) techniques. Moreover, the field emission scanning electron microscopic (FESEM) and transmission electron microscopic (TEM) techniques are performed to study the surface morphology of the as-synthesized specimens. The as-prepared ternary nanohybrid showed a reduced optical band gap (~ 1.92 eV) evaluated through Ultraviolet–Visible (UV–Vis) absorbance spectra. From the current density–voltage (J–V) characteristics, the *Ohmic* conductance ~ 0.126 S was found for the ternary nanohybrid PIN/PPY/CdS. In addition, the ternary nanohybrid exhibits comparatively the higher PL intensity which indicates the higher electron–hole recombination rate. All these results indicate the aptness of the as-synthesized PIN/PPY/CdS nanohybrid towards optoelectronic device application.

Graphic Abstract



Keywords Polyindole · Polypyrrole CdS nanoparticles · UV–Visible · Photoluminescence · Optoelectronics

Extended author information available on the last page of the article

1 Introduction

In the era of optoelectronic nanotechnology, organic–inorganic nano-structured hybrid materials have played significant role in developing more convenient devices such as organic light emitting diodes (OLEDs), organic field effect transistors (OFETs), photovoltaic cells and photodetectors [1–3]. The inorganic nanocrystals incorporated organic polymer matrices are known as organic–inorganic nanohybrids. The main aim of developing these nanohybrids to enhance the properties such as mechanical strength, thermal stability, chemical stability as well as optical and electrical properties of their individual components [4]. The organic polymer matrix has metallic properties, structural flexibility, optical conductivity, flexible electronic properties. However, the inorganic nanocrystals deliver high charge carrier mobility, adjustable band gap, thermal stability, mechanical stability, dielectric and magnetic properties [5, 6]. There are some additional enriched characteristics occurred owing to proper interfacial interaction between polymeric matrix and nanocrystals. Thus, organic–inorganic nanohybrids reveal excellent optical, electrical, mechanical and thermal properties due to new functionalities. These surprising results of organic–inorganic nanohybrid materials give significant contribution in the various applications such as organic light emitting diodes (OLEDs), organic photovoltaic cell (OPVs), organic field effect transistors (OFETs) and many more optoelectronic applications [7–9]. Byoung Hoon Lee et al. reported graphene based conducting polymer hybrid transparent electrode for organic optoelectronic device application [10]. Kandulna et al. reported PMMA-TiO₂ nanocomposite as electron transport layer for OLED application [11].

Conducting polymers (CPs) or *sp*² hybridized conjugated polymers have become the main pillar in developing impactful nanohybrid materials due to their thermal, electrical, optical as well as mechanical properties [12]. In recent years, CPs have considered as most promising candidates for flexible supercapacitor application due to their specific properties such as high-redox activity, high intrinsic flexibility and most importantly high conductivity [13, 14]. There are some well-known CPs such as polyaniline (PANI), polypyrrole (PPY), polyindole (PIN), polythiophene and their derivatives received great attention towards an area of research in the optoelectronic field because of their extensive electrical conductivity, low ionization potential, low energy optical transitions, high electron affinity as well as low synthesis cost [15, 16].

Among of these, the PIN can be effortlessly synthesized by oxidation technique and exhibit good thermal

stability, moderate degradation rate, high redox activity and tunable electrical conductivity [17]. Owing to these unique properties, PIN matrix has been recognized as the most substantial polymer matrix for versatile applications [17–19]. Also, PPY exhibits excellent electrical conductivity with light weight and low cost of synthesis [20–22]. Currently, some researchers have reported excellent aptness of organic–inorganic nanohybrid material based on the composite polymer matrix. Singh et al. have reported the biomimetic synthesis of organic–inorganic hybrid based on PANI-Polyethylene glycol-CdS [23]. Tiwari et al. presented the synthesis of composite polymer PPY/PANI and showed their enriched thermal stability [24]. Wilson et al. reported the synthesis of ternary nanocomposite PPY–PANI–Au using electrochemical deposition technique for the application of DNA sensing [25]. Verma et al. also reported the ternary nanocomposite PANI/PPY/CdS as an electron transport layer for the OLED application [26]. Kandulna et al. illustrated electron transport properties of PANI/PPY/ZnO nanocomposites for the OLED applications [27]. Choudhary et al. synthesized PPY–TiO₂–rGO nanocomposite as electron transport layer for OLEDs [28]. Recently, Verma et al. have published the optoelectronic properties of ternary nanohybrid based on polyindole, cadmium sulphide CdS and reduced graphene oxide [29].

The embodiment of inorganic nanocrystals (metal sulfide/oxide) such as PbS, ZnS, CdS, MoS₂, ZnO, SnO₂, and TiO₂ into CPs matrices, aiming to enhance their properties. All of these, CdS nanocrystals have some excellent optical and electrical properties which are apt for optoelectronic applications [30]. Recently, Chenglong Hu et al. have reported the optical properties of CdS nanoparticle based multi-walled carbon nanotubes for optoelectronic devices [31].

On the basis literature survey, it was observed that the numerous arrangements of organic conjugated polymers including polyindole, polypyrrole and inorganic nanocrystals including CdS as well as reduced graphene oxide have been reported for the various applications. But, to the best of our knowledge the synthesis of ternary nanohybrid PIN/PPY/CdS and their optoelectronic properties have never reported yet.

In this communication, research work is focused on the development of ternary nanohybrid resulting from the incorporation of CdS nanoparticles into binary polymeric matrix PIN/PPY using in situ oxidative polymerization technique. In addition, the comparative study of optoelectronic properties has done with the binary nanohybrids PIN/CdS and PPY/CdS which concluded that the PIN/PPY/CdS nanohybrid may become apt material for optoelectronic device application.

2 Experimental

2.1 Materials

Indole (99% pure), pyrrole (99.98% pure), cadmium nitrate tetrahydrate (98% pure), sodium sulfide flakes (extra pure) and ammonium persulfate (APS) (98% pure). These chemicals were purchased from Merck Pvt. Limited and used for the desired synthesis. As a solvent deionised (DI) water was used throughout the synthesis process.

2.2 Synthesis of Binary PIN/CdS and PPY/CdS Nanohybrids

PIN/CdS and PPY/CdS both binary nanohybrids were synthesized via in-situ oxidative polymerization technique. 1.25 g indole was dissolved into 50 mL of DI water with constant stirrer at 80 °C temperature. In other hand as-synthesized 0.25 g of CdS nanoparticles [26] (20% of indole) were dispersed into 30 mL of DI water. After 40 min dispersed CdS nanoparticles were added into the indole solution with continuous stirring for 1 h. Then after above indole–CdS solution was shifted into an ice bath and 20 mL of APS (2.5 g) solution was added dropwise into indole–CdS mixture with constant stirrer. APS acts as an oxidizing agent to initiate the polymerization process. After 6–8 h, polymerization process is completed and the product was obtained in violet colour which was filtered out.

For the preparation of PPY/CdS nanohybrid, 0.65 g pyrrole and 0.13 g as-synthesized CdS nanoparticles (20% of pyrrole) were dispersed into 70 mL DI water with continuous stirring for 1 h at room temperature. Afterward, synthesis procedure is similar to PIN/CdS as discussed above. In this synthesis resultant filtered product was obtained in dark black color. Both PIN/CdS and PPY/CdS products were washed with DI water and ethanol to remove impurities. The filtered precipitates were dried in vacuum oven at 65 °C for 24 h so as to obtain PIN/CdS and PPY/CdS nanohybrid. Similarly neat PIN and neat PPY matrices were synthesized in absence of CdS nanoparticles.

2.3 Synthesis of Ternary PIN/PPY/CdS Nanohybrids

Indole, pyrrole monomers and as synthesized CdS nanoparticles were taken in the ratio of 10:5:1 for the synthesis of PIN/PPY/CdS ternary nanohybrid. 1.25 g indole monomer was dissolved into 40 mL of DI water with constant stirrer at 80 °C temperature. 0.65 g pyrrole and 0.13 g as-synthesized CdS nanoparticles (20% of pyrrole) were dispersed into 40 mL DI water with continuous stirring at room temperature. After 1 h indole solution was added into pyrrole–CdS

reaction mixture and then transferred into ice bath. At the same time 20 mL of APS (2.5 g) solution was added dropwise into indole–pyrrole–CdS mixture with constant stirrer. APS acts as an oxidizing agent to initiate the polymerization process. After 6–8 h, polymerization process is completed and product was obtained in black colour which was filtered out and washed with DI water and ethanol several times to remove additional oxidant and monomers. The obtained residue was dried in vacuum oven at 65 °C for 30 h to obtain final PIN/PPY/CdS composite. Schematic route for synthesis of PIN/PPY/CdS nanohybrid have been shown in Fig. 1.

2.4 Material Characterizations

In order to examine the crystalline structure of the as-synthesized specimens, X-ray diffraction (XRD) technique (XPRT-Pro with Cu-K α radiations) was performed and corresponding XRD patterns were recorded in the 2 θ range 10°–70°. The molecular bonds and functional groups as present in the specimens were identified using Fourier-transform infrared (FTIR) spectroscopy (Perkin Elmer-RX1). For the FT-IR analysis samples were prepared using a KBr pellet technique and FT-IR spectra were recorded in the range 4000–500 cm⁻¹. The field emission scanning electron microscopic (FESEM) (SUPRA-55 Carl ZEISS Germany) and transmission electron microscopic (TEM) (TECNAI G2, 20 TWIN) techniques were used for the study of surface morphology. UV–Visible spectroscopic (UV-2450, Shimadzu Asia Pacific) technique was carried out to study the optical properties, absorbance spectra of the as synthesized specimens were recorded in the range 200–800 nm. At the excitation energy of 344 nm photoluminescence (PL) emission spectra were recorded using fluorescence spectrophotometer (F-2500 Hitachi). Dielectric properties of the as synthesized specimens were examined by LCR meter (HIOKI-353250). Moreover, in order to examine electrical properties J–V characteristics had been done using KEITHLEY 2400 source meter.

3 Result and Discussions

3.1 XRD and FT-IR Analysis

The XRD patterns for as-synthesized specimens have been revealed in the Fig. 2a. The XRD pattern for CdS nanoparticles showed three distinct peaks at 2 θ values of 26.4°, 43.83° and 52.17° ascribed to the crystal planes (111), (220) and (311), respectively [32] according to JCPDS 98-008-6103. These crystal planes define the cubic phase of CdS nanoparticles [33, 34]. However, the XRD patterns of both neat PIN and neat PPY showed a broad band between 2 θ = 19.4° to 26.4° which indicate the amorphous nature of polyindole

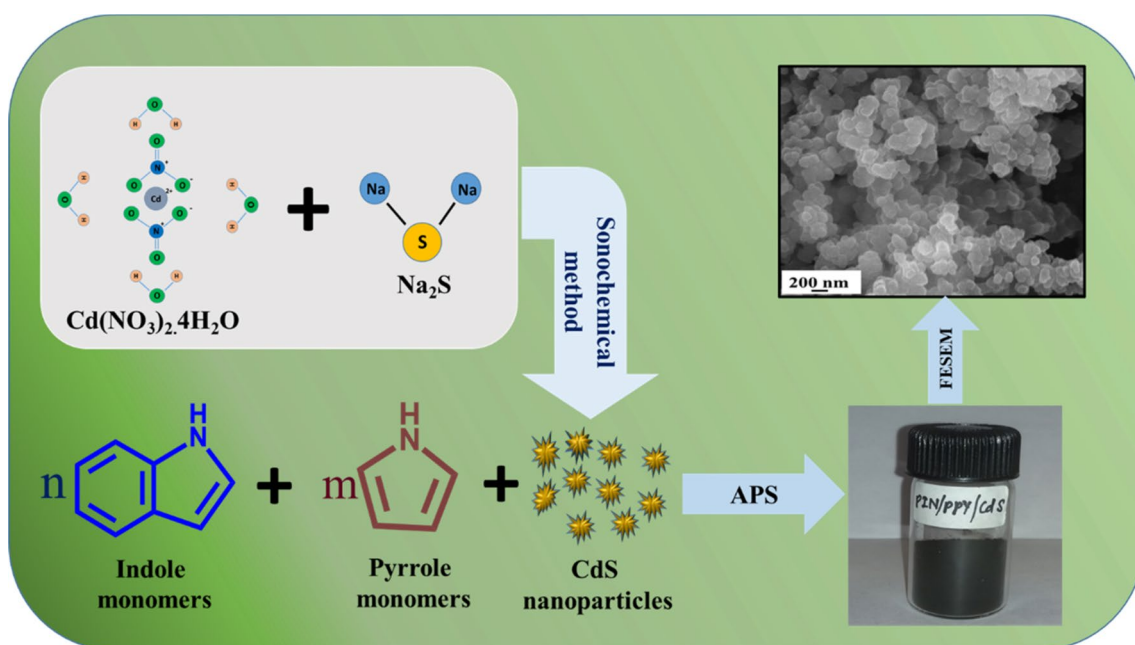
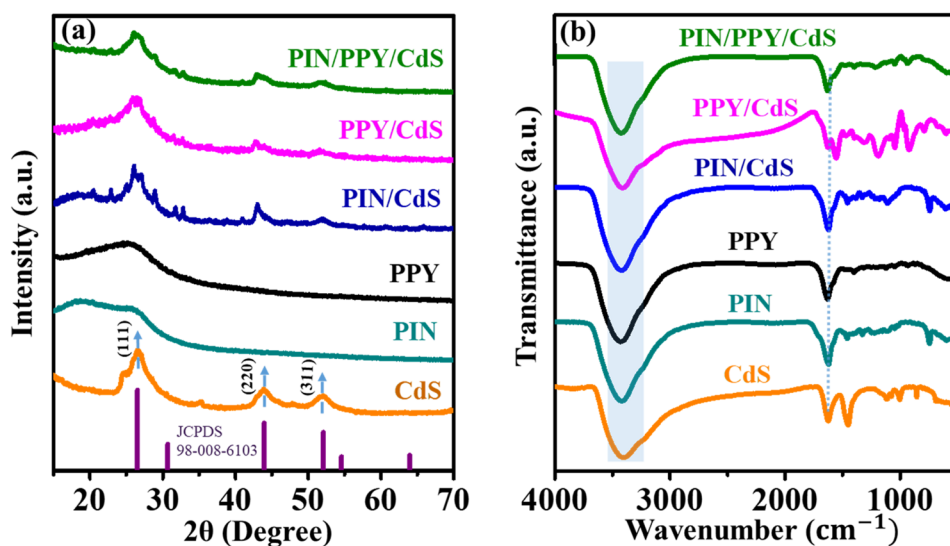


Fig. 1 Schematic route for laboratory synthesis of polyindole/polypyrrole/CdS ternary nanohybrid

Fig. 2 a X-ray diffraction patterns and **b** Fourier transform infrared spectra of polyindole, polypyrrole, cadmium sulfide and their binary and ternary nanocomposites



and polypyrrole [35, 36]. In case of PIN/CdS nanohybrid, three peaks appeared at $2\theta = 26.2^\circ$, 42.47° and 52.56° indicate the crystalline nature of nanohybrids due to the incorporation of CdS nanoparticles. In case of PPY/CdS and PIN/PPY/CdS nanohybrids, similar peaks were appeared as present in CdS nanoparticles. The appearance of these peaks in nanohybrids due to the incorporation of CdS nanoparticles clearly indicate the crystalline behaviour of nanohybrids and also confirm the successful integration of CdS nanoparticles into PIN as well as PPY matrix.

The FT-IR spectroscopic technique was performed to ascertain the bond stretching between the functional groups

as present in the specimens. As seen in Fig. 2b, CdS showed a strong interaction with water as revealed by reflected peaks located at 3412 cm^{-1} and 1631 cm^{-1} owing to O–H stretching and O–H bending modes [37]. However, both neat PIN and PIN/CdS nanohybrid exhibited nearly similar FTIR spectra having peaks positioned at 3425 cm^{-1} , 1634 cm^{-1} , 1453 cm^{-1} , and 743 cm^{-1} relegated to N–H stretching, C–C stretching, C–N stretching vibration and out-of-plane deformations for C–H bond respectively [15, 38]. The additional peak occurred in PIN/CdS around at 1103 cm^{-1} owing to the incorporation of CdS nanoparticles affirms the interaction between CdS nanoparticles and PIN matrix. In case of

neat PPY and PPY/CdS nanohybrid, FT-IR spectra exhibited similar peaks at 3425 cm^{-1} and 1634 cm^{-1} as found in PIN matrix owing to common functional groups. PPY/CdS showed some additional peaks in the wavenumber range 1321 cm^{-1} to 527 cm^{-1} associated with the interaction between CdS nanoparticles to PPY matrix. Moreover, ternary nanohybrid PIN/PPY/CdS also revealed the transmittance peaks at 3425 cm^{-1} , 1634 cm^{-1} attributed to the N–H and C–C stretching. In PIN/PPY/CdS nanohybrid some peaks as found in PIN and PPY matrix are merged and take new places at 937 cm^{-1} , 1045 cm^{-1} and 1211 cm^{-1} which affirms the successful interaction between polymer matrices and CdS nanoparticles.

3.2 FESEM Analysis

The FESEM technique was employed to study the surface morphological properties of the as-synthesized specimens and corresponding FESEM images have been shown in Fig. 3a–f. The FESEM image for CdS nanoparticles reveals the granular agglomerated morphology (Fig. 3a) and the average diameter of the CdS nanoparticles was found around 24 nm. As seen in Fig. 3b, pure PIN exhibits randomly interconnected bulbous like morphology. However, the surface morphology of pure PPY shows spherical granular like structure (Fig. 3c) similarly as obtained in our previous work [26]. The FESEM image for binary nanohybrid PIN/CdS revealed the incorporation of CdS nanoparticles into the PIN matrix by showing mixed irregular agglomerated like morphology as shown in Fig. 3d. From the figure, it is also clear that CdS nanoparticles were bound tightly by PIN matrix. In case of PPY/CdS nanohybrid, CdS nanoparticles entirely mixed into PIN matrix and obtained resultant morphology with reduced particle size in comparison to the pure PPY as seen in Fig. 3e. Moreover, ternary nanohybrid PIN/PPY/CdS revealed that the mixed morphology as in the shape of pure PPY by reducing particle size owing to the strong interaction between inorganic CdS and within two polymeric matrices.

3.3 TEM Analysis

TEM technique was performed to the as-prepared ternary nanohybrid PIN/PPY/CdS for the study of in-depth surface morphology. Figure 4 showed the TEM image of PIN/PPY/CdS nanohybrid at 200 nm. The particle size of PIN matrix reduced on the embodiment of PPY matrix. CdS nanoparticles as incorporated into PIN/PPY matrix can be recognized by dark patches as seen by a yellow circle. However, PIN/PPY matrix can be recognized by light gray colour as indicated by the green arrow. The uniform distribution of black patches is the witness of a proper embodiment of CdS nanoparticles into PIN/PPY matrix. The results as seen in

the TEM technique are the well agreement to the outcomes as obtained during FESEM analysis.

3.4 Ultraviolet–Visible Analysis and Evaluation of Optical Band Gap

Ultraviolet–Visible (UV–Vis) absorbance spectra for as-synthesized specimens were studied to explore the optical parameter such as optical band gap, refractive index and optical conductivity. The UV–Visible spectra and corresponding graphs for optical band gap have been shown in Fig. 5a–d.

In order to evaluate the optical band gap (E_g) for the as-synthesized PIN, PIN/CdS and PIN/PPY/CdS nanohybrids, the absorption coefficients (α) were extracted through their respective absorption spectra by the following equation:

$$\alpha = \frac{2.303A}{d} \quad (1)$$

where, A is the absorbance and d, thickness of the specimens ($\sim 0.175\text{ mm}$). Then curves between $(\alpha hv)^2$ and hv have plotted using following Touc's relation [39].

$$\alpha hv = A(hv - E_g)^n \quad (2)$$

Here, hv , is photon energy and n represents the density of states which may take values $1/2$, $3/2$, 2, 3 corresponding to direct allowed, direct forbidden as well as indirect allowed, indirect forbidden optical band gap respectively. The values of direct optical band gap for PIN, PIN/CdS and PIN/PPY/CdS nanohybrids, were evaluated by Tauc's plot between $(\alpha hv)^2$ and hv . It was found that the value of optical band gap for PIN matrix reduces as CdS nanoparticles were incorporated into them. The value of pure PIN was calculated as 2.33 eV, however reduced optical band gap 2.14 eV was obtained for PIN/CdS. Furthermore, the value of the optical band gap reduces to 1.81 eV when PPY was embedded into PIN/CdS nanohybrid. The reduction of optical band gap value in nanohybrids is mainly attributed to the addition of intermediate transition bands between conduction bands and valence bands within PIN matrix. The values of optical band gap for synthesized specimens were listed in the Table 1.

3.5 J–V Characteristics

The current density (J) vs. voltage (V) characteristics were measured using the fore probe method by applying a varying voltage (V) to obtain the corresponding current density (J). In order to prepare the sample for performing the J–V characteristics, the as-synthesized specimens were spin coated on the ITO glass plate of 1 cm^2 . The ohmic conductance and ohmic resistance were calculated from the J–V characteristics as displayed in Fig. 6.

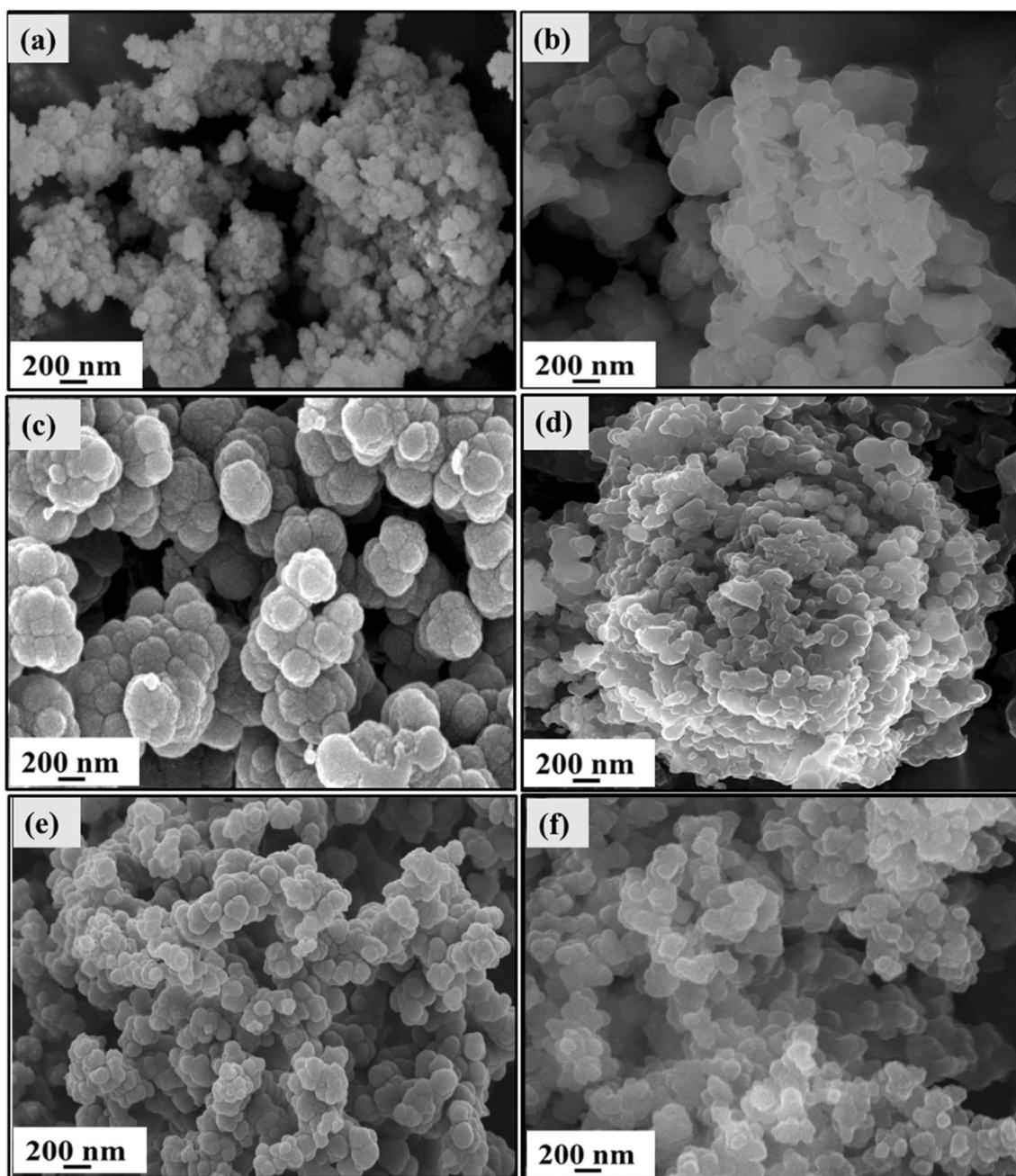


Fig. 3 FESEM images for **a** CdS nanoparticles, **b** Neat polyindole (PIN), **c** Neat polypyrrole (PPY), **d** polyindole/CdS, **e** polypyrrole/CdS binary nanohybrids and **f** polyindole/polypyrrole/CdS ternary nanohybrid

The current density–voltage (J–V) characteristics of the as-synthesized specimens viz. neat PIN, CdS nanoparticles, PIN/CdS and PIN/PPY/CdS nanohybrids were recorded in the voltage range -10 V to $+10$ V as presented in Fig. 6. Ohmic resistance was calculated from the slope of J–V characteristics and hence the reciprocal of ohmic resistance gives the values of ohmic conductance. It was observed that the values of electrical conductance varied as: neat PIN < CdS nanoparticles < PIN/CdS < PIN/PPY/CdS nanohybrids. The

ohmic conductance (0.016 S) of PIN matrix was enhanced up to 0.069 S on the integrating CdS nanoparticles into PIN matrix. Furthermore, the addition of PPY into PIN/CdS nanohybrid, heightens the conductivity of PIN up to 0.12 S. The augmentation in electrical conductivity is mainly attributed to the formation of new additional conducting channels within nanohybrids. The ohmic resistance and conductance as evaluated by J–V characteristics have been listed in Table 2.

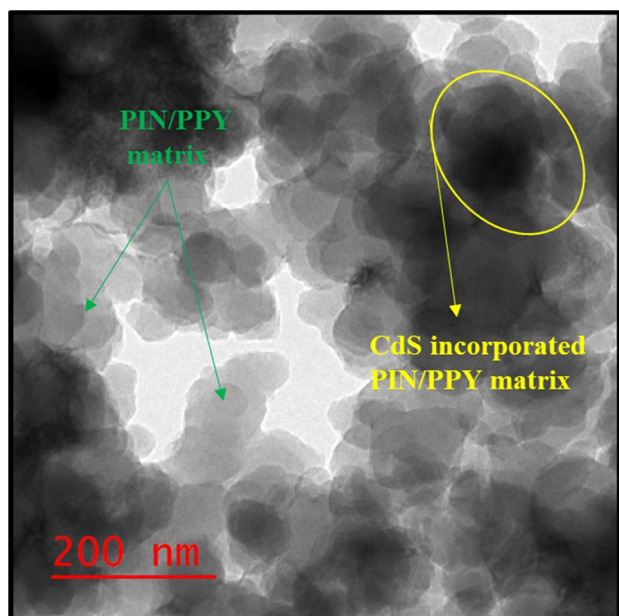


Fig. 4 Transmission electron microscopic (TEM) image of ternary polyindole/polypyrrole/CdS (PIN/PPY/CdS) nanohybrid at 200 nm Scale

3.6 Photoluminescence (PL) Analysis

The photoluminescence refers as a light emission phenomenon based on the electron–hole (e^-h^+) recombination during the interaction of light energy to the material [40]. The

PL emission spectra for CdS nanoparticles, PIN/CdS and PIN/PPY/CdS nanohybrids at excitation wavelength 344 nm have been recorded in the wavelength range 425–770 nm as shown in Fig. 7. There were three major peaks obtained for CdS, PIN/CdS as well as PIN/PPY/CdS nanohybrids in the visible region located at 468 nm, 583 nm, and 716 nm corresponding to blue, yellow and red band respectively. A peak with low intensity also appeared corresponding to red band. It was observed that PL intensity of ternary nanohybrid PIN/PPY/CdS attains comparatively maximum intensity. Since PL intensity is directly proportional to the e^-h^+ recombination rate so in ternary nanohybrid PIN/PPY/CdS maximum e^-h^+ recombination occurred which make suitable candidate for optoelectronic device material [11, 41].

4 Conclusion

We conclude the successful incorporation of CdS nanoparticles into neat PIN, neat PPY and binary PIN/PPY matrix, affirmed by XRD and FT-IR analysis. The uniform distribution of CdS nanoparticles over polymeric matrices was confirmed by FESEM and TEM analysis. The as-prepared ternary nanohybrid exhibits a reduced optical band gap (~ 1.92 eV) evaluated through UV–Visible spectra. The enhancement in optical conductivity of the ternary nanohybrid has found to 44.62% in comparison to pure PIN matrix. Also, the nanohybrid exhibits comparatively the higher PL intensity which indicates the higher

Fig. 5 **a** Ultraviolet–Visible spectra, optical band gap so obtained for **b** Neat polyindole (PIN) matrix, **c** Polyindole/cadmium sulfide (PIN/CdS) binary nanohybrid and **d** Polyindole/polypyrrole/cadmium sulphide (PIN/PPY/CdS) ternary nanohybrids

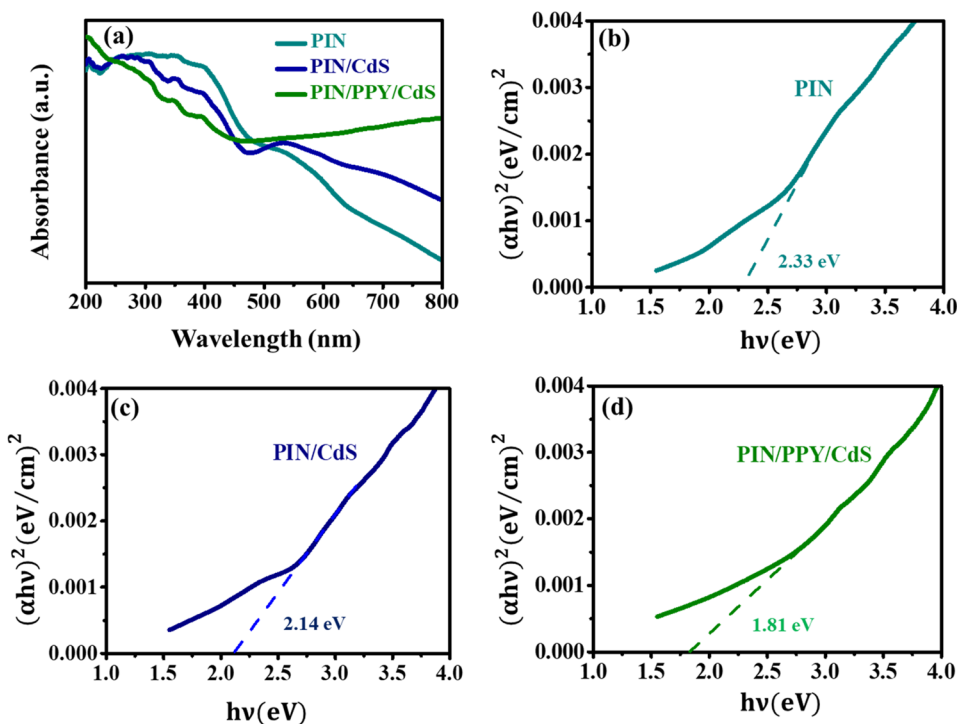


Table 1 Optical band gap evaluated by Ultraviolet–Visible absorbance spectra for neat polyindole, binary polyindole/cadmium sulfide and ternary polyindole/polypyrrole/cadmium sulfide nanohybrids

Specimens	Optical band gap (eV)
PIN	2.28
PIN/CdS	2.11
PIN/PPY/CdS	1.92

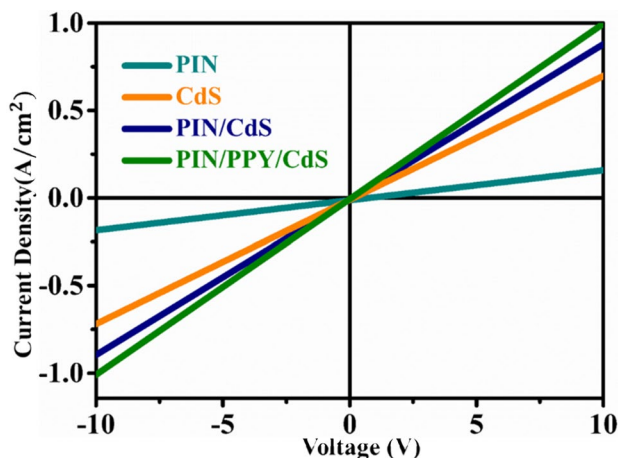


Fig. 6 Current density–Voltage (J–V) characteristic plots for polyindole, cadmium sulfide and their binary and ternary nanocomposites with polypyrrole

Table 2 Ohmic resistance and ohmic conductance for neat polyindole, cadmium sulfide nanoparticles, binary polyindole/cadmium sulfide and ternary polyindole/polypyrrole/cadmium sulfide nanohybrids

Specimens	Ohmic resistance (Ω)	Ohmic conductance (S)
PIN	62.5	0.016
CdS	14.49	0.069
PIN/CdS	11.49	0.087
PIN/PPY/CdS	7.93	0.126

electron–hole recombination rate and higher *Ohmic* conductance ~ 0.126 S. The augmentation in the results as obtained from the analysis of optoelectronic properties for the as-synthesized PIN/PPY/CdS nanohybrid infers it as a prominent candidate for optoelectronic device application.

Acknowledgements Authors want to express thanks to Indian institute of technology (Indian school of mines), Dhanbad, India for financial support and acknowledge DST Project No. SR/FST/PSI-004/2013 for PL spectrometer.

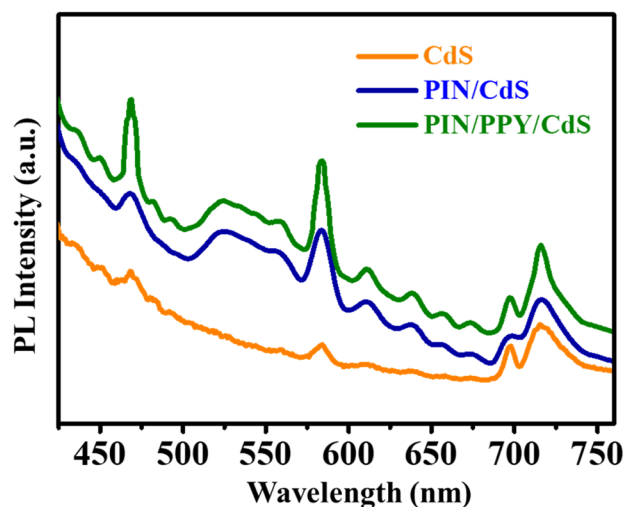


Fig. 7 Photoluminescence spectra for cadmium sulfide (CdS) nanoparticles, polyindole/cadmium sulfide (PIN/CdS) binary nanohybrid and polyindole/polypyrrole/cadmium sulfide (PIN/PPY/CdS) ternary nanohybrid

References

1. T.-P. Nguyen, Surf. Coat. Technol. **206**, 742 (2011)
2. W. Zhu, X.-L. Chen, J. Chang, R.-M. Yu, H. Li, D. Liang, X.-Y. Wu, C.-Z. Lu, J. Mater. Chem. C **6**, 7242 (2018)
3. Z. Li, J. Kong, F. Wang, C. He, J. Mater. Chem. C **5**, 5283 (2017)
4. C. Sanchez, B. Julián, P. Belleville, M. Popall, J. Mater. Chem. **15**, 3559 (2005)
5. H. Mudila, P. Prasher, M. Kumar, A. Kumar, M.G.H. Zaidi, A. Kumar, Mater. Renew. Sustain. Energy **8**, 9 (2019)
6. J.Q.M. Almarashi, M.H. Abdel-Kader, J. Inorg. Organomet. Polym. Mater. (2020). <https://doi.org/10.1007/s10904-020-01482-0>
7. Z. Shu, E. Beckert, R. Eberhardt, A. Tünnermann, J. Mater. Chem. C **5**, 11590 (2017)
8. G. Xu, Q. Xu, A. Qin, J. Cheng, N. Wang, J. Wei, C. Zhang, Z. Yang, B.Z. Tang, J. Mater. Chem. C **1**, 1717 (2013)
9. R. Kandulna, R.B. Choudhary, Polym. Bull. **75**, 3089 (2018)
10. B.H. Lee, J.-H. Lee, Y.H. Kahng, N. Kim, Y.J. Kim, J. Lee, T. Lee, K. Lee, Adv. Funct. Mater. **24**, 1847 (2014)
11. R. Kandulna, R.B. Choudhary, R. Singh, B. Purty, J. Mater. Sci. Mater. Electron. **29**, 5893 (2018)
12. M. Shaban, M. Rabia, A.M.A. El-Sayed, A. Ahmed, S. Sayed, Sci. Rep. **7**, 14100 (2017)
13. I. Shown, A. Ganguly, L.-C. Chen, K.-H. Chen, Energy Sci. Eng. **3**, 2 (2015)
14. A. Singh, Z. Salmi, P. Jha, N. Joshi, A. Kumar, P. Decorse, H. Lecoq, S. Lau-Truong, D.K. Aswal, S.K. Gupta, M.M. Chehimi, RSC Adv. **3**, 13329 (2013)
15. R. Perveen, Inamuddin, S. ul haque, A. Nasar, A.M. Asiri, G.M. Ashraf, Sci. Rep. **7**, 13353 (2017)
16. A. Mekki, N. Joshi, A. Singh, Z. Salmi, P. Jha, P. Decorse, S. Lau-Truong, R. Mahmoud, M.M. Chehimi, D.K. Aswal, S.K. Gupta, Org. Electron. **15**, 71 (2014)
17. P. Sireesha, R. Sasikumar, S.-M. Chen, C. Su, P. Ranganathan, S.-P. Rwei, Appl. Surf. Sci. **423**, 147 (2017)
18. W. Wang, S. Wu, Appl. Surf. Sci. **396**, 1360 (2017)
19. E. Dogan, E. Ozkazanc, H. Ozkazanc, Synth. Met. **256**, 116154 (2019)

20. A. Madani, B. Nessark, R. Boukherroub, M.M. Chehimi, J. Electroanal. Chem. **650**, 176 (2011)
21. A. Yeole, T. Sen, D.P. Hansora, S. Mishra, J. Appl. Polym. Sci. **132**, 42379 (2015)
22. N. Hakimi, A. Zouaoui, F.Z. Satour, A. Sahari, A. Zegadi, J. Inorg. Organomet. Polym. Mater. **30**, 330 (2020)
23. A. Singh, N.P. Singh, R.A. Singh, Bull. Mater. Sci. **34**, 1017 (2011)
24. D.C. Tiwari, R. Jain, S. Sharma, J. Appl. Polym. Sci. **110**, 2328 (2008)
25. J. Wilson, S. Radhakrishnan, C. Sumathi, V. Dharuman, Sensors Actuators B **171–172**, 216 (2012)
26. A. Verma, R.B. Choudhary, J. Inorg. Organomet. Polym. Mater. **29**, 444 (2019)
27. R. Kandulna, R.B. Choudhary, Optik (Stuttg). **144**, 40 (2017)
28. R.B. Choudhary, R. Kandulna, Mater. Sci. Semicond. Process. **94**, 86 (2019)
29. A. Verma, R.B. Choudhary, Mater. Sci. Semicond. Process. **110**, 104948 (2020)
30. T.K. Das, S. Prusty, Polym. Plast. Technol. Eng. **51**, 1487 (2012)
31. C. Hu, Y. Wang, S. Chen, H. Cheng, M. Lin, Y. Zhang, D. He, X. Liu, J. Liu, RSC Adv. **6**, 78053 (2016)
32. A. Rafiq, M. Imran, M. Aqeel, M. Naz, M. Ikram, S. Ali, J. Inorg. Organomet. Polym. Mater. (2019). <https://doi.org/10.1007/s10904-019-01343-5>
33. P. Rodríguez, N. Muñoz-Aguirre, E.S.-M. Martínez, G. Gonzalez, O. Zelaya, J. Mendoza, Appl. Surf. Sci. **255**, 740 (2008)
34. A. Bouzidi, I.S. Yahia, W. Jilani, H. Guermazi, S. AlFaify, H. Algarni, J. Inorg. Organomet. Polym. Mater. **28**, 1494 (2018)
35. R.B. Choudhary, A. Verma, Opt. Mater. (Amst). **96**, 109310 (2019)
36. M. Irfan, A. Shakoor, J. Inorg. Organomet. Polym. Mater. **30**, 1287–1292 (2019)
37. S. García-Carvajal, D. Hernández-Martínez, I. Linzaga-Elizalde, J.L. Maldonado, P. Altuzar-Coello, M.E. Nicho, Eur. Polym. J. **116**, 471 (2019)
38. P. Chhattise, K. Handore, A. Horne, K. Mohite, A. Chaskar, S. Dallavalle, V. Chabukswar, J. Chem. Sci. **128**, 467 (2016)
39. P.B. Rathod, S.A. Waghuley, J. Appl. Spectrosc. **83**, 586 (2016)
40. D. Nayak, R.B. Choudhary, Opt. Mater. (Amst). **91**, 470 (2019)
41. P.F. Ji, Y. Li, Y.L. Song, F.Q. Zhou, M.L. Tian, S.Q. Yuan, Phys. Lett. A **383**, 125841 (2019)

Publisher's Note Springer Nature remains neutral with regard to jurisdictional claims in published maps and institutional affiliations.

Affiliations

Ajeet Verma¹ · Ram Bilash Choudhary¹ · Debashish Nayak¹ · Gobind Mandal¹

✉ Ram Bilash Choudhary
rbcism@gmail.com

¹ Nanostructured Composite Materials Laboratory,
Department of Applied Physics, Indian Institute
of Technology (Indian School of Mines), Dhanbad 826004,
India